Organic & Biomolecular Chemistry

Cite this: *Org. Biomol. Chem.*, 2011, **9**, 7705

www.rsc.org/obc

PAPER

Insights into molecular recognition of Lewis^X mimics by DC-SIGN using NMR and molecular modelling†

Cinzia Guzzi,[a] Jesús Angulo,[a] Fabio Doro,[b] José J. Reina,[b] Michel Thépaut,[c,d,e] Franck Fieschi,[c,d,f] Anna Bernardi,[b] Javier Rojo[a] and Pedro M. Nieto*[a]

Received 10th June 2011, Accepted 31st August 2011
DOI: 10.1039/c1ob05938f

In this work, we have studied in detail the binding of two α-fucosylamide-based mimics of Lewis^X to DC-SIGN ECD (ECD = extracellular domain) using STD NMR and docking. We have concluded that the binding mode occurs mainly through the fucose moiety, in the same way as Lewis^X. Similarly to other mimics containing mannose or fucose previously studied, we have shown that both compounds bind to DC-SIGN ECD in a multimodal fashion. In this case, the main contact is the interaction of two hydroxyl groups one equatorial and the other one axial (O3 and O4) of the fucose with the Ca^{2+} as Lewis^X and similarly to mannose-containing mimics (in this case the interacting groups are both in the equatorial position). Finally, we have measured the K_D of one mimic that was 0.4 mM. Competitive STD NMR experiments indicate that the aromatic moiety provides additional binding contacts that increase the affinity.

Introduction

DC-SIGN (Dendritic Cell-Specific ICAM-3 Grabbing Non-integrin) also named CD209, is a C-type lectin present mainly on the surface of immature dendritic cells.[1] This protein shows a short intracellular domain, a transmembrane domain, and an extracellular region containing a neck ending in a Carbohydrate Recognition Domain (CRD) at the C-terminus. This CRD is responsible for the interaction with highly glycosylated structures present at the surface of several pathogens such as viruses (HIV, SIV, Hepatitis C), bacteria, yeasts, and parasites.[2] DC-SIGN plays a key role in the infection processes of some of these pathogens, which are recognized by interactions of the lectin with carbohydrate structures from pathogens' glycoproteins (gp120, GP1, *etc.*).[1,2]

Thus, the development of small-molecule mimics of oligosaccharides capable of inhibiting sugar-binding by this lectin is attracting the attention as a way to develop drugs with good stability and synthetic availability.[3,4]

Natural ligands of DC-SIGN consist of mannose oligosaccharides such as high mannose, or fucose-containing Lewis-type determinants. In all cases, the binding occurs in a Ca^{2+} dependent manner.[5–7] Many experimental and modelling studies from different groups have demonstrated that the Lewis oligosaccharides are rigid and compact structures with the fucose ring stacked on top of the galactose residue.[8] Moreover, the conformation of Lewis^X carbohydrate determinants **1** (Fig. 1) bound to antibodies was found to be extremely similar to that observed for the free oligosaccharides. Thus, the recognition and binding of the Lewis^X carbohydrates by their protein partners does not induce significant conformational changes.[8]

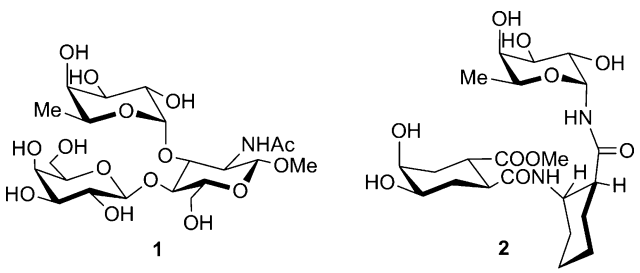

Fig. 1 Structure of Lewis^X(OMe), **1** and first fucose-based mimic **2**.

Previous studies established that α-fucosylamides are functional mimics of enzymatically and chemically labile α-fucosides. Some of us described the first fucose-based unnatural ligand of DC-SIGN **2** (Fig. 1),[9] an interesting candidate to prepare improved compounds or multivalent systems able to block the lectin with high affinity. Indeed, this ligand was found to be a better inhibitor for DC-SIGN than the natural Lewis^X.[9]

[a]*Glycosystems Laboratory, Instituto de Investigaciones Químicas, CSIC-US, Americo Vespucio, 49 41092 Sevilla, Spain. E-mail: pedro.nieto@iiq.csic.es; Fax: +34 954460595; Tel: +34 954489568*
[b]*Universita' degli Studi di Milano, Dipartimento di Chimica Organica e Industriale and CISI, via Venezian 21, 20133 Milano, Italy*
[c]*Institut de Biologie Structurale, Université Grenoble I, 41 rue Jules Horowitz, 38027 Grenoble, France*
[d]*CNRS, UMR 5075 Grenoble, France*
[e]*CEA, Grenoble, France*
[f]*Institut Universitaire de France, 103 boulevard Saint-Michel, 75005, Paris, France*

† Electronic supplementary information (ESI) available. See DOI: 10.1039/c1ob05938f

As an improvement of this glycomimetic compound **2**, a library of potential new mimetics have been prepared and evaluated as inhibitors of DC-SIGN using biosensors.[10] From this library, we have selected two of the most active ligands, **3** and **4**, containing the same α-fucosylamide anchor used in **2**, and an aromatic ring to take advantage of potential CH–π interactions.[11,12] We have performed a full analysis of their interaction with the ECD of DC-SIGN (Fig. 2),[10] by NMR and computational techniques. Ligand binding was analysed mainly by Saturation Transfer Difference (STD) NMR spectroscopy, one of the most widespread NMR methods, together with transfer NOE, to characterize binding interactions between small ligands and macromolecular receptors.[13]

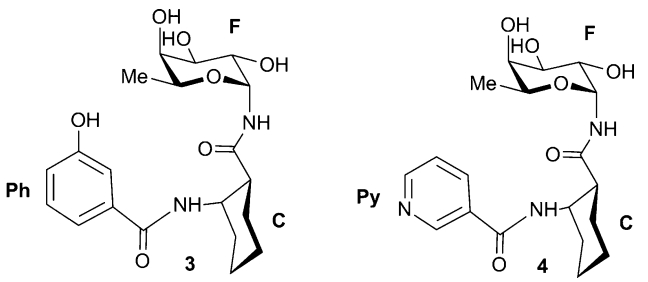

Fig. 2 New fucose-based glycomimetic ligands containing an α-fucosylamide anchor and an aromatic ring.

In addition, we have investigated the existence of multiple binding modes using the CORCEMA-ST protocol (Complete Relaxation and Conformational Exchange Matrix), a useful tool for analysing the STD data and obtaining STD-based epitope mapping on a quantitative basis.[14,15]

Results and discussion

The two mimics studied, **3** and **4** (Fig. 2), belong to a library of fucosylamides compounds, designed as potential ligands for DC-SIGN ECD.[10] They have been chosen based on previous studies and binding affinity data obtained by SPR. They differ only in the aromatic ring and they have been selected in order to evaluate the influence of the aromatic moiety on affinity.

Structural analysis of the free ligands 3 and 4

Both compounds are rather flexible systems and the α-glycosyl amides are poorly parameterized in available force fields for molecular mechanics calculations. However, coupling constant analysis and NOESY spectra allowed us to restrict the range of possible conformations of the ligands in solution (see ESI† and Fig. 3). This conformational analysis reproduced the experimental data observed for free ligands **3** and **4**. Due to the structural and spectral similarities between both ligands, the focus of the computational study in the free-state is just on one of the compounds (mimic **3**).

In a first step, a conformational analysis of the central ring was performed based on NMR data. Experimental coupling constants of mimic **3**, determined by homonuclear decoupling, revealed a single conformation of the *cis*-β-aminoacid (**C** ring), in which the carbonyl group is in the equatorial position, and the amino group in the axial one (see ESI†), as already determined in previous studies for the parent compound (**2**).[9]

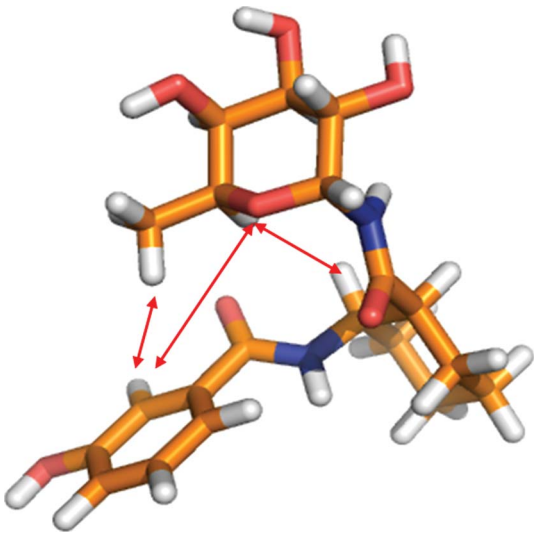

Fig. 3 Representative conformer of **3** showing key NOE cross peaks.

Monte Carlo Multiple Minimum (MCMM)[16] conformational searches and mixed mode MC/SD dynamics simulations[17] were performed using Macromodel-AMBER*,[18–20] MM3*[21,22] and OPLS_2005[23] force fields combined with the GB/SA water solvation model.[24] In the case of AMBER*, while all conformers presented the chair conformation of the **C** ring, in agreement with the experimental *J*-coupling constant, only one structure showed interatomic distances consistent with the experimental NOE results. Conformers arising from MM3* multiple minimization, showed interatomic distances in agreement with NOE data, but also showed a number of low energy solutions inconsistent with the **C** ring chair conformation determined from coupling constants. Although a more realistic ensemble could be obtained disallowing ring opening, the best agreement was obtained using the OPLS_2005 force field. Both, multiple minimization[18] and dynamics gave rise to conformers whose conformation of the **C** ring and interprotonic distances fit well with the experimental ones (Table 1).

Due to the similar structures of compounds **3** and **4**, we assumed the same reasoning for compound **4** and therefore a comparable free conformation was accepted (see NOESY spectra in ESI†).

Conformational analysis of the bound ligands

Structural analysis of the ligand–receptor complexes. In the presence of the lectin, the sign of NOE cross peaks become inverted indicating ligand–protein binding at a favourable rate (Fig. 4). Furthermore, the key inter residue NOE signals described above (Table 1) are stronger in the presence of the receptor (trNOE). In general, with the exception of the peaks' intensities and sign, no major differences appeared between the NOE fingerprints for free and bound ligand **3** (Fig. 4). This indicates that the lectin recognizes the conformation of the oligosaccharide that corresponds to the main conformation existing in solution.[25] In addition, trROESY experiments were also recorded in order to identify false trNOEs due to spin-diffusion effects[26,27] and the spectra confirmed the trNOE peaks.

Table 1 Calculated and experimental inter-proton distances (Å) for mimic 3 in comparison with key NOE contacts

Proton pair	MC/SD Distance (Å)[a]			MC+MC/SD Distance (Å)[b]			Experimental Distances (Å)[c]	NOE intensity
	MM3*	AMBER*	OPLS 2005	MM3*	AMBER*	OPLS 2005		
H-1 F/H-1 C	4.5	4.5	4.3	4.4	4.5	4.3	3.8	—
H-5 F/H-5 C	3.8	4.5	3.1	3.1	5.3	2.9	3.4	weak
H-5 F/H-2 Ph	6.1	5.3	6.7	5.6	4.7	6.5	—	—
H-5 F/H-6 Ph	3.8	4.0	4.5	4.1	3.7	4.2	3.9	very weak
H-5 F/H-2 Ph	3.9	4.2	4.5	4.0	3.8	4.2	3.8	weak
Me F/H-2 Ph	4.4	5.6	4.1	4.1	5.7	3.4	3.9	medium
Me F/H-5 Ph	5.2	5.7	5.7	4.7	5.1	5.4	—	very weak
Me F/H-6 Ph	4.3	5.5	4.2	4.2	5.8	3.6	4.0	weak

[a] Distances evaluated from $<r^{-6}>^{-1/6}$ monitored during the simulation. [b] Distances obtained from MD minimized snapshots, calculated as average of the $<r^{-6}>$ of the individual conformations accessible in the first 3 kcal mol^{-1}. [c] Distances derived using the isolated spin-pair approximation (ISPA) by comparing relative NOE intensities.

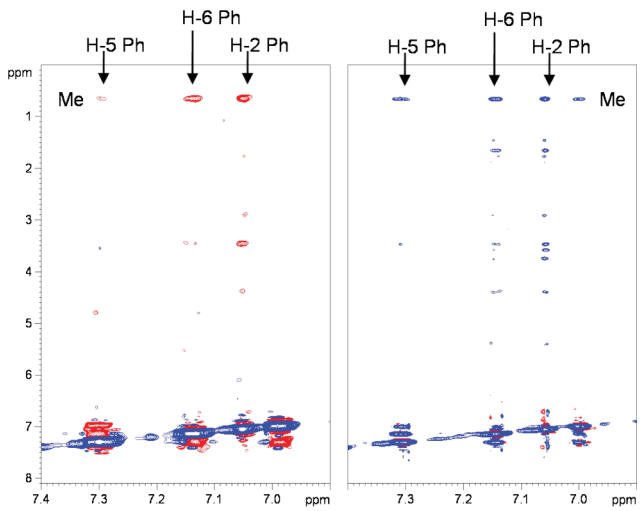

Fig. 4 Expansions of NOESY experiments at 500 ms of mimic **3**, free (left), and in the presence of 19 μM of DC-SIGN ECD (right), showing some key NOE peaks. The Me–H-4 Ph NOE peak was also observable in the free state (left), but close to the noise level (not shown).

A working model for the structure of DC-SIGN in complex with mimic **3** was obtained by docking studies starting from the PDB structure of human DC-SIGN (pdb entry 1SL5).[7] The X-ray crystal structure was modified removing all crystallographic water molecules except W13 and W36, since previous studies identified two hydrophilic areas with favourable energy occupied by these water molecules.[28] The role of water molecules in the binding between lectins and glycosylated ligands is a matter of current interest because of their potential contribution to the ligand–receptor binding.[29,30]

One of the starting ligand structures used for docking was the global minimum from the multiple minimization of the ligand discussed above. A rigid docking (see ESI†) was performed by superimposing the fucose ring of mimic **3** with the fucose residue of Lewis^X as it is in the crystallographic structure (pdb entry 1SL5). A semi-flexible docking was performed by Glide (Grid-Based Ligand Docking with Energetics),[31–34] while ligand conformational flexibility is handled by a conformational search.

All docked poses generated appeared to maintain the interactions between the Ca^{2+} atom and two hydroxyl groups of the fucose residue, predominantly groups OH-3 and OH-4. Only one of the poses was able to explain the key interresidue NOE signals experimentally observed (Fig. 3 and 4). Nevertheless, in this case QM-docking yielded worse results than standard docking. The structure in Fig. 5 has been selected from the previous results using the experimental data as a filter.

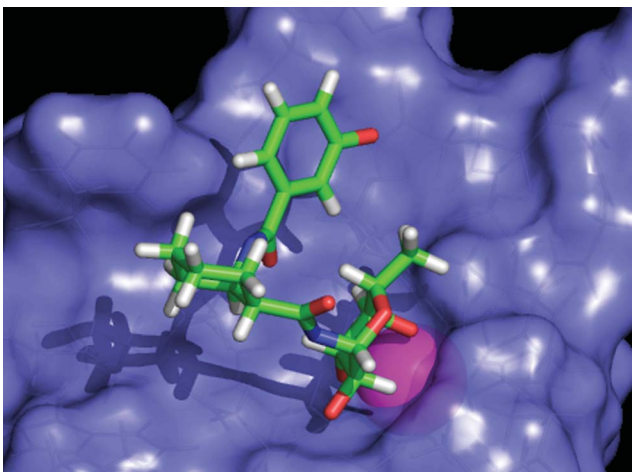

Fig. 5 Best docking pose of mimic **3** in the binding pocket of DC-SIGN as selected by semi-flexible docking taking into account the experimental evidence (Schrodinger, Inc.).

The STD experiments confirm the theoretical data, both compounds interact mostly through the fucose residue that binds a Ca^{2+} atom, an additional contribution from aromatic signals is detected for **3** and **4**, and other weaker signals from the cyclohexyl ring are also observed (Fig. 6). This is consistent with the hairpin-like shape of the molecules in which the central ring is far from the surface of the protein, the aromatic ring is interacting with Phe-313 while the fucose is interacting with Ca^{2+} by two adjacent hydroxyl groups (see Fig. 5 and 6).

Based on experimental evidence, among all docked poses obtained, we chose only one from the semi-flexible docking (Fig. 5). This complex was our starting point to apply the CORCEMA-ST protocol in order to predict the STD intensities based on the topology of the molecular models.[14,15] From the docked pose which presents the coordination between the Ca^{2+} atom and hydroxyl

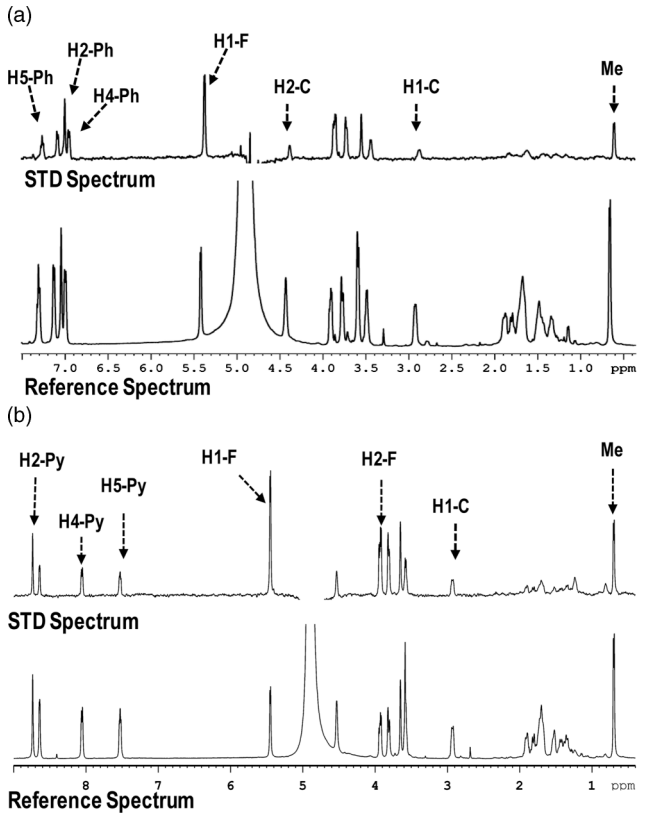

Fig. 6 STD and reference spectra of a) mimic **3** (1 mM) and b) mimic **4** (1 mM) in the presence of DC-SIGN ECD (19 μM) at 10 °C, 500 MHz. Protons belonging to phenol ring (Ph), pyridine ring (Py), fucose (F, Me) and to cyclohexyl ring (C) are labelled.

groups 3 and 4 of fucose (model O3–O4), we built three other models of interaction and minimized them using MacroModel (models O4–O3, O2–O3 and O3–O2, for nomenclature see ESI†).

In CORCEMA-ST the simplified expression for the observable magnetization $\mathbf{I}(t)$ in a STD experiment is given by eqn (1)[14,15]

$$\mathbf{I}(t) = \mathbf{I}_0 + [1 - \exp\{-\mathbf{D}t\}]\mathbf{D}^{-1}\mathbf{Q} \quad (1)$$

We have calculated STD intensities of different protons in the ligand of the four complexes and compared them with the experimental values (ESI†).[35] None of the individual solutions satisfied all the experimental data. However, combinations of several association modes could be feasible assuming the existence of multiple binding modes. Nevertheless, in terms of qualitative ranking of STD intensities within ligand protons, a main contribution of the structure O3–O4 is strongly suggested.

STD NMR epitope mapping. We performed STD NMR experiments, at different saturation times of Lewis^X **1** and mimics **3** and **4**, in the presence of 19 μM of DC-SIGN (ECD) which exists in solution as a tetramer.[36]

For all three compounds, fucose protons H-1 F, H-2 F, H-3 F receive the largest amount of saturation indicating a common binding mode in which these protons are very close to the protein. In all cases F-1 receives the major amount of magnetization. Protons H-4 F, H-5 F and the methyl group are also involved in binding but show smaller STD. This confirms that the interaction with the lectin occurs mainly through the fucose residue[7] consistent with the expected binding mode.[9] On the other hand, for mimics **3** and **4**, the observation of STD signals belonging to protons H-1 and H-2 of the C ring, indicates that the fucosylamide anchor makes close contacts with the protein. In addition, signals corresponding to the aromatic moiety were evident in the STD spectra of the mimics, indicating a further interaction of this ring with the ECD of DC-SIGN (Fig. 6).

We characterized the binding epitope using relative STD intensities, as introduced by Mayer and Meyer[37] (Fig. 7) and the analysis of initial growth, proposed by Mayer and James.[38] Using this approach the slope corresponds to the STD intensity in the absence of T_1 bias. Thus, the experimental curves were fitted to an exponential function described by the equation: STD (t_{sat}) = $STD_{max}(1 - \exp(-k_{sat}t_{sat}))$ which allows us to calculate STD at zero saturation time (STD_0) by the resulting parameters STD_{max} and k_{sat}.[38] These STD_0 were then used to calculate the binding epitope independently of T_1 and rebinding effects.[39]

The results demonstrate that the fucose based ligands bind the protein mimicking the recognition of known natural ligands as the Lewis^X antigen, this is, through the fucose residue, while the aromatic rings in the mimics provide additional contact points with DC-SIGN (Fig. 6 and 7).

K_D determination by STD NMR

In order to obtain the dissociation constant (K_D) of **3** we used a protocol based on STD NMR, recently developed in our group.[39] This method allows direct measurements of receptor–ligand dissociation constants (K_D) from single-ligand titration

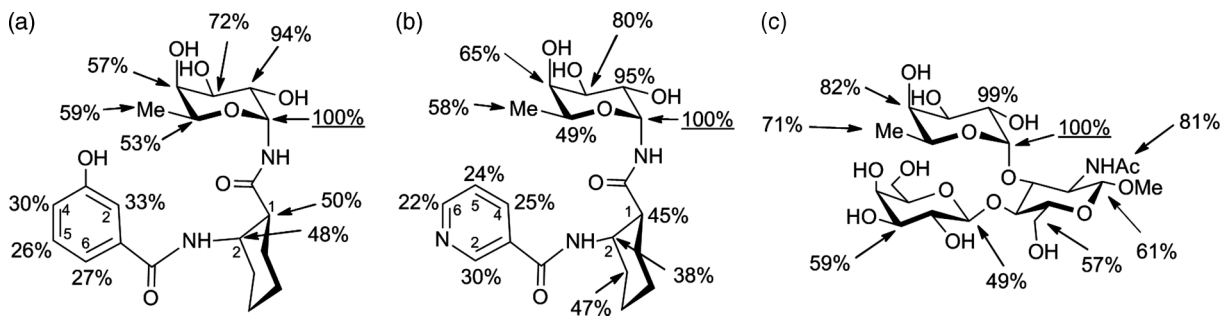

Fig. 7 Relative values of STD amplification factors for a) mimic **3** b) mimic **4** c) Lewis^X **1**. Ligand concentration 1 mM, DC-SIGN ECD 19 μM, in 500 μL buffer D_2O (150 mM NaCl, 4 mM $CaCl_2$, 25 mM d-Tris, pD 8). The ratio of intensities I_{STD}/I_0 was normalized using the largest STD effect (anomeric proton H-1 of the Fucose residue (100%) as a reference).

experiments, by constructing the binding isotherms using the initial growth rates of the STD amplification factors (STD-AF_0). STD NMR titration experiments for mimic **3** (concentrations 0.2, 0.5, 1, 2, 4 mM) were performed at 800 MHz and 25 °C in the presence of 19 μM of DC-SIGN ECD. The K_D, obtained as an average of different selected ligand protons, was 0.4 (± 0.1) mM, (Fig. 8).

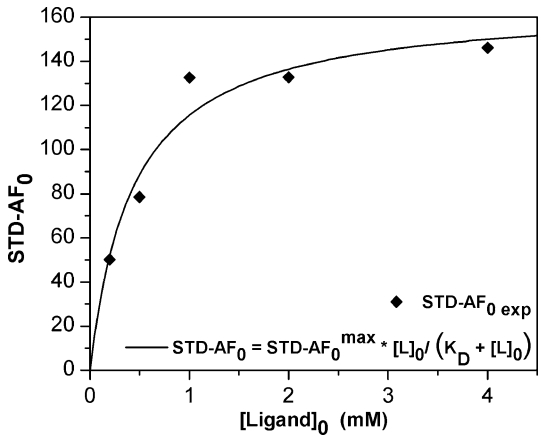

Fig. 8 K_D determination based on STD NMR using the binding isotherm of STD-AF_0 initial growth rates approach.[39]

STD NMR competition experiments

Since it is known that the binding process of DC-SIGN to fucose-containing Lewis^X carbohydrates and to high mannose glycans, $(Man)_9(GlcNAc)_2$, is based on specific interactions,[36,40] we wanted to analyse the competition between Lewis^X(OMe), α-Man($OCH_2CH_2N_3$), and mimic **4**, by STD NMR. The solid state data strongly suggest that the recognition site is the same in all cases. Thus, a decrease on the STD magnitude upon addition of the second ligand would confirm the competition for the same binding site.

First, we measured the competition of mannose derivative with mimic **4** (Fig. 9, a), as well as with Lewis^X(OMe) (Fig. 9, b). In both cases there was a decrease in STD intensity after addition of 1 mM of α-Man($OCH_2CH_2N_3$), showing that mannose was capable of displacing both, mimic **4** and Lewis^X (**1**) and, therefore, the three ligands compete for the same binding site, corroborating that we are detecting their specific interactions with DC-SIGN, by STD NMR.

Concerning the competition experiment between Lewis^X(OMe) and mimic **4**, the results confirmed, as expected, a competition for the same site of interaction, and evidenced a higher relative affinity of mimic **4** in comparison to the natural ligand. Indeed, the STD growth curves belonging to Lewis^X(OMe) protons showed a greater decrease when competing with mimic **4** than in competition with mannose derivative (Fig. 9, b). Thus, it can be concluded from this experiment that **4** is a stronger DC-SIGN binder than Lewis^X or mannose.

Finally, we carried out competition experiments between mimics **3** and **4**. To that aim, we prepared a sample containing both ligands at the same concentration, in the presence of 19 μM of DC-SIGN (ECD). As we could differentiate some of the signals of protons belonging to each mimic, we were able to integrate the intensities

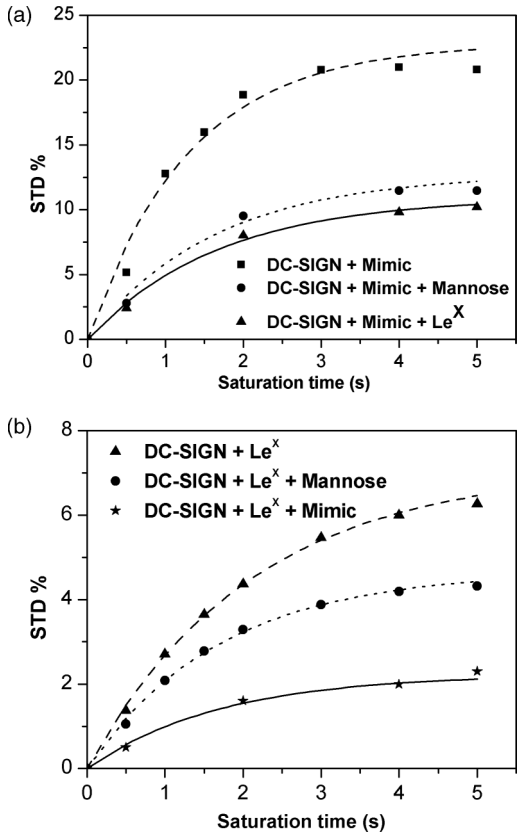

Fig. 9 STD NMR competition experiments. STD growth curves of a) the proton H-1 of fucose of **4** (squares), in the presence of mannose (circles), or Lewis^X(OMe) 1 (triangles); b) the proton H-Ac of *N*-acetyl-glucosamine of **1** (triangles), in the presence of mannose (circles), or **4** (stars).

of STD signals for each proton independently. The corresponding STD growth curves obtained for the two mimics were comparable and, in consequence, DC-SIGN should have the same affinity for both ligands within experimental error (Fig. 10). These results are in agreement with SPR inhibition data.[10]

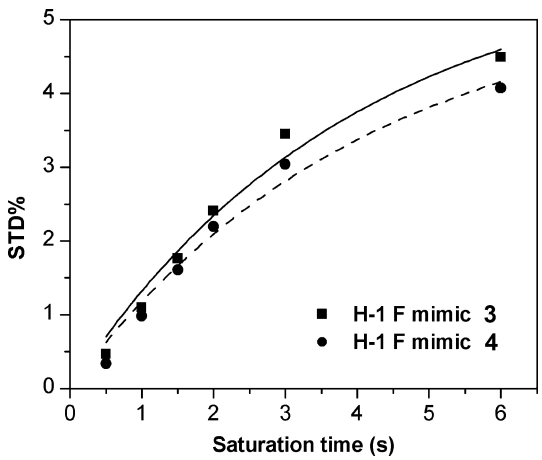

Fig. 10 STD NMR competition experiments between **3** and **4**. STD growth curves belonging to H-1 of fucose in mimic **3** (squares) and mimic **4** (circles).

Conclusions

We have studied the binding of two fucose-containing mimics **3** and **4** and Lewis^X **1** to DC-SIGN (ECD) by NMR and molecular modelling. In all cases, NMR reveals that, despite their flexibility, there are little or no significant structural changes on the ligand upon binding in terms of change of conformation. Remarkably, these Lewis^X and fucosyl glycomimetics **3** and **4** are recognised by DC-SIGN using the same binding site that recognises mannose derivatives, as seen in previous NMR or X-ray studies. This is sustained by STD competition experiments between mimic **4**, Lewis^X **1**, and α-Man($OCH_2CH_2N_3$), which showed a decrease in the STD signals when the second ligand was added. These compounds have a global common shape that lead to a common binding mode where the fucose interacts with Ca^{2+} using two adjacent hydroxyl groups; glucosamine or cyclohexyl rings are pointing towards the outside; and galactose or aromatic rings are oriented back to the DC-SIGN binding site. These experiments additionally concluded that the better binder in those experimental conditions were both mimics. We have interpreted this result as the ability of the aromatic ring to replace the Gal moiety establishing new interactions, which have been confirmed in STD experiments (Fig. 6 and 7).

This observation is of great interest for the design of new DC-SIGN inhibitors as the substitution of the galactose ring by the aromatic moiety simplifies and shortens the synthesis of the ligands without affecting the affinity for the lectin. This has been demonstrated by the determination of the K_D value of **3** which was within the same range of the natural antigen Lewis^X.

The STD NMR quantitative analysis indicates that binding of glycomimetics **3** and **4** is multimodal, and that several ligand orientations can be recognised by the lectin, as we have previously demonstrated in the case of DC-SIGN (ECD) binding by mannose-containing inhibitors.[41] Further multimodal analysis will be considered in order to obtain a precise characterization of the orientations of the ligands into the DC-SIGN binding pocket.

Experimental section

NMR spectroscopy

NMR spectroscopy experiments were performed on Bruker Digital Avance 800 MHz and DRX 500 MHz spectrometers equipped with 5 mm inverse triple-resonance probes. NMR samples were prepared in 500–600 μL of 99.9% D_2O. For the experiments with the receptor (DC-SIGN ECD 19 μM), the receptor was produced as previously described,[42] and concentrated at 19 μM after dialysis in buffer: D_2O (150 mM NaCl, 4 mM $CaCl_2$, 25 mM d-Tris, pD = 8). Different concentrations of ligands were used depending on the experiments: 2 mM for complete assignment of the signals, 1 mM for epitope mapping and competition experiments and 0.2, 0.4, 1.0, 2.0 and 4.0 mM (titration experiments) for K_D determination. Distances in Table 1 were calculated using the Tropp equation when adequate.

STD NMR experiments were carried out at 10 and 25 °C by using a train of Gaussian shaped pulses of 49 ms and with an interpulse delay of 1 ms.[43] Saturation times to obtain the STD buildup curves were 0.5, 1, 1.5, 2, 3, 4 and 5 s. The on-resonance frequency was set to −0.5 or −1 ppm, whereas off-resonance frequency was 40 ppm. Blank experiments were performed to assure the absence of direct saturation to the ligand protons.

NOESY experiments were performed with a relaxation delay of 1.5 s, using a phase sensitive pulse program with gradient pulses in mixing time and with presaturation.[44,45]

To determine K_D the binding isotherms were constructed from initial slopes of STD amplification factors (STD-AF_0) calculated at every ligand concentration along the titration. The value of STD-AF_0 was obtained by fitting the STD-AF evolution with the saturation time to the equation

$$\text{STD-AF}(t) = a(1 - \exp(-bt))^{38}$$

as the product of the coefficients ab. The STD-AF_0 values were then plotted as a function of the concentration of ligand, and the resulting isotherm of initial slopes was mathematically fitted to a Langmuir equation to obtain the dissociation constant.[46]

Computational methods

All calculations were run using the Schrödinger suite of programs through the Maestro 9.0 graphical interface.[47] Conformational search was performed by using the MacroModel/Batchmin[24] package and the AMBER* force field[19,20] (Kolb's parameters were used for the hydroxy acid moiety)[48] and MM3* force field[21,22] by using 10 000 steps of the Monte Carlo Multiple Minimum method (MCMM).[16] Bulk water solvation was simulated by using generalized Born GB/SA continuum solvent model.[49] Truncated Newton conjugate gradient (TNCG) procedure, extended cut-off distances (equivalent to a van der Waals cut-off of 8.0 Å, an electrostatic cut-off of 20.0 Å and a H-bond cut-off of 4.0 Å), were used.

The MC/SD[17] dynamic simulations, were run with AMBER*, MM3* and OPLS_2005 force fields.[18,23] All simulations were performed at 300 K, with a dynamic time step of 1–1.5 fs and a ratio of SD to MC of 1. Convergence was checked by monitoring both energetic and geometrical parameters.

Protein setup: Starting from the X-ray crystal structure (resolution = 1.80 Å) of human DC-SIGN complex, (pdb entry 1SL5; complex of DC-SIGN CRD and lacto-*N*-fucopentaose III (Fucα 1,3-(Galβ 1,4)-GlcNAc 1,3-Galβ) (LNFPIII), a molecular model of the protein was prepared. The crystal structure of 1SL5 (pdb structure) was modified by removing all the waters of crystallization except W13 and W36,[28,30,50] hydrogens were added using Maestro.[47] The preparation of the protein was performed using the methodology previously described by Bernardi's group.[28] The complex structure coming from the 1SL5 pdb entry was minimized with the OPLS-2005 force field and using the convergence method Truncated Newton Conjugate Gradients, with coordinates of Ca^{2+} atom and the oxygens of the water 13 and 36 in the binding site fixed to their crystallographic positions.

Docking

The previous structure was employed as receptor in the docking studies in the Grid generation and as reference structure. An "enclosing box" with dimensions of 36 Å and a partial charge cut off of 0.25 were set. No constraints were established to allow the ligand to explore freely the bounding box.

Then for the ligand docking we defined the core pattern comparison with the heavy atoms of fucose and the hydroxyls coordinating the calcium ion, based on experimental data.[51] A tolerance of 3.5 Å was set, in order to ensure the maximum conformational freedom of the fucose moiety while preserving the interaction fucose-Ca^{2+} and to allow different binding modes involving the hydroxyl groups O2–O3 or O3–O4.

Starting from the same minimized complex and using the previous Grid file, further structural models for the interaction of the mimic **3** (global minimum) with DC-SIGN were generated by QM-Polarized docking protocol of Glide.[34] This protocol aims to improve the partial charges on the ligand atoms in a Glide docking run by replacing them with charges derived from quantum mechanical calculations on the ligand in the field of the receptor.

CORCEMA-ST

The three-dimensional structures employed for the full relaxation matrix calculations were based on the crystallographic structure of the complex of human DC-SIGN with Lewis^X (pdb 1SL5) and prepared as already discussed. For each structure, hydrogen atoms were added and energy minimization was applied using Maestro 9.0.[47] All exchangeable hydrogen atoms were excluded in the calculations, as the STD NMR experiments were performed in D_2O. Assuming a spherical shape for the protein tetramer, the correlation time of bound ligand was set to 144 ns whereas we chose a value of 0.5 ns for the free ligand correlation time and a value of 10 ps for the methyl group internal correlation time. To reduce the dimensions of the matrices, a cut off of 8 Å from the ligand was used. The STD intensities for each binding mode were calculated as percentage fractional intensity changes ($\mathbf{S}_{calc,k} = (([(\mathbf{I}_{0k} - \mathbf{I}(t)_k)100]/\mathbf{I}_{0k})$, were **k** is a particular proton in the complex, and $\mathbf{I}_{0k}$ its thermal equilibrium value) from the intensity matrix $\mathbf{I}(t)$,[14] and the calculation was carried out for the set of saturation times experimentally measured (0.5, 1, 1.5, 2, 3, 4 and 5 s). From the resulting STD build-up curves, a mathematical fitting to a monoexponential equation ($STD(t_{sat}) = STD_{max}(1 - \exp(-k_{sat}t_{sat}))$)[38] was done, and the initial slope STD_0^{calc} was obtained. The theoretical STD values were compared to experimental ones using the NOE *R*-factor[35,52] defined as:

$$\sqrt{\frac{\Sigma W_k (STD_{0,k}^{exp} - STD_{0,k}^{calc})^2}{\Sigma W_k (STD_{0,k}^{exp})^2}} \quad (2)$$

In the eqn (2) $STD_{0,k}^{exp}$ and $STD_{0,k}^{calc}$ refer to experimental and calculated initial slopes STD_0 for proton **k**.

Acknowledgements

Support of this work for funding by EU (PITN-GA-2008-213592, CARMUSYS), MICINN (CTQ2009-07168) and (CTQ2008-01694) and MEC (ITCS-2009-43 for access to 800 MHz on LRB) are gratefully acknowledged. We thank also for European FEDER funds. J.A. and C.G. acknowledge MICINN for a Ramón y Cajal contract and EU for a Marie Curie Fellowship respectively. We also acknowledge to Dr J. M. de la Fuente for providing a sample of **1**.

Notes and references

1 T. B. H. Geijtenbeek, R. Torensma, S. J. van Vliet, G. C. F. van Duijnhoven, G. J. Adema, Y. van Kooyk and C. G. Figdor, *Cell*, 2000, **100**, 575–585.
2 Y. van Kooyk and T. B. H. Geijtenbeek, *Nat. Rev. Immunol.*, 2003, **3**, 697–709.
3 A. Bernardi and P. Cheshev, *Chem.–Eur. J.*, 2008, **14**, 7434–7441.
4 P. Sears and C. H. Wong, *Angew. Chem., Int. Ed.*, 1999, **38**, 2301–2324.
5 B. J. Appelmelk, I. van Die, S. J. van Vliet, C. Vandenbroucke-Grauls, T. B. H. Geijtenbeek and Y. van Kooyk, *J. Immunol.*, 2003, **170**, 1635–1639.
6 E. van Liempt, C. M. C. Bank, P. Mehta, J. J. Garcia-Vallejo, Z. S. Kawar, R. Geyer, R. A. Alvarez, R. D. Cummings, Y. van Kooyk and I. van Die, *FEBS Lett.*, 2006, **580**, 6123–6131.
7 Y. Guo, H. Feinberg, E. Conroy, D. A. Mitchell, R. Alvarez, O. Blixt, M. E. Taylor, W. I. Weis and K. Drickamer, *Nat. Struct. Mol. Biol.*, 2004, **11**, 591–598.
8 E. Yuriev, W. Farrugia, A. M. Scott and P. A. Ramsland, *Immunol. Cell Biol.*, 2005, **83**, 709–717.
9 G. Timpano, G. Tabarani, M. Anderluh, D. Invernizzi, F. Vasile, D. Potenza, P. M. Nieto, J. Rojo, F. Fieschi and A. Bernardi, *ChemBioChem*, 2008, **9**, 1921–1930.
10 M. Andreini, D. Doknic, I. Sutkeviciute, J. J. Reina, J. Duan, E. Chabrol, M. Thepaut, E. Moroni, F. Doro, L. Belvisi, J. Weiser, J. Rojo, F. Fieschi and A. Bernardi, *Org. Biomol. Chem.*, 2011, **9**, 5778–5786.
11 A. Bernardi, D. Arosio, D. Potenza, I. Sanchez-Medina, S. Mari, F. J. Canada and J. Jimenez-Barbero, *Chem.–Eur. J.*, 2004, **10**, 4395–4406.
12 S. Vandenbussche, D. Diaz, M. Carmen Fernandez-Alonso, W. Pan, S. P. Vincent, G. Cuevas, F. Javier Canada, J. Jimenez-Barbero and K. Bartik, *Chem.–Eur. J.*, 2008, **14**, 7570–7578.
13 B. Meyer and T. Peters, *Angew. Chem., Int. Ed.*, 2003, **42**, 864–890.
14 V. Jayalakshmi and N. R. Krishna, *J. Magn. Reson.*, 2004, **168**, 36–45.
15 N. R. Krishna and V. Jayalakshmi, *Prog. Nucl. Magn. Reson. Spectrosc.*, 2006, **49**, 1–25.
16 G. Chang, W. C. Guida and W. C. Still, *J. Am. Chem. Soc.*, 1989, **111**, 4379–4386.
17 F. Guarnieri and W. C. Still, *J. Comput. Chem.*, 1994, **15**, 1302–1310.
18 *MacroModel*, version 9.7, Schrödinger-LLC, New York, NY.
19 H. Senderowitz, C. Parish and W. C. Still, *J. Am. Chem. Soc.*, 1996, **118**, 8985–8985.
20 H. Senderowitz and W. C. Still, *J. Org. Chem.*, 1997, **62**, 1427–1438.
21 N. L. Allinger, Y. H. Yuh and J. H. Lii, *J. Am. Chem. Soc.*, 1989, **111**, 8551–8566.
22 N. L. Allinger, M. Rahman and J. H. Lii, *J. Am. Chem. Soc.*, 1990, **112**, 8293–8307.
23 G. A. Kaminski, R. A. Friesner, J. Tirado-Rives and W. L. Jorgensen, *J. Phys. Chem. B*, 2001, **105**, 6474–6487.
24 F. Mohamadi, N. G. J. Richards, W. C. Guida, R. Liskamp, M. Lipton, C. Caufield, G. Chang, T. Hendrickson and W. C. Still, *J. Comput. Chem.*, 1990, **11**, 440–467.
25 J. J. Lundquist and E. J. Toone, *Chem. Rev.*, 2002, **102**, 555–578.
26 S. R. Arepalli, C. P. J. Glaudemans, G. D. Daves, P. Kovac and A. Bax, *J. Magn. Reson., Ser. B*, 1995, **106**, 195–198.
27 J. L. Asensio, F. J. Canada and J. Jimenez-Barbero, *Eur. J. Biochem.*, 1995, **233**, 618–630.
28 F. Doro, Bachelor Degree Thesis, 2009, University of Milan.
29 C. Clarke, R. J. Woods, J. Gluska, A. Cooper, M. A. Nutley and G. J. Boons, *J. Am. Chem. Soc.*, 2001, **123**, 12238–12247.
30 A. Almond, *Carbohydr. Res.*, 2005, **340**, 907–920.
31 R. A. Friesner, J. L. Banks, R. B. Murphy, T. A. Halgren, J. J. Klicic, D. T. Mainz, M. P. Repasky, E. H. Knoll, M. Shelley, J. K. Perry, D. E. Shaw, P. Francis and P. S. Shenkin, *J. Med. Chem.*, 2004, **47**, 1739–1749.
32 M. Agostino, C. Jene, T. Boyle, P. A. Ramsland and E. Yuriev, *J. Chem. Inf. Model.*, 2009, **49**, 2749–2760.
33 *Glide*, version 5.5, Schrödinger-LLC, New York, NY.
34 A. E. Cho, V. Guallar, B. J. Berne and R. Friesner, *J. Comput. Chem.*, 2005, **26**, 915–931.
35 Y. Xu, I. P. Sugar and N. R. Krishna, *J. Biomol. NMR*, 1995, **5**, 37–48.
36 D. A. Mitchell, A. J. Fadden and K. Drickamer, *J. Biol. Chem.*, 2001, **276**, 28939–28945.
37 M. Mayer and B. Meyer, *J. Am. Chem. Soc.*, 2001, **123**, 6108–6117.
38 M. Mayer and T. L. James, *J. Am. Chem. Soc.*, 2004, **126**, 4453–4460.
39 J. Angulo, P. M. Enriquez-Navas and P. M. Nieto, *Chem.–Eur. J.*, 2010, **16**, 7803–7812.

40 H. Feinberg, D. A. Mitchell, K. Drickamer and W. I. Weis, *Science*, 2001, **294**, 2163–2166.
41 J. Angulo, I. Diaz, J. J. Reina, G. Tabarani, F. Fieschi, J. Rojo and P. M. Nieto, *ChemBioChem*, 2008, **9**, 2225–2227.
42 G. Tabarani, M. Thepaut, D. Stroebel, C. Ebel, C. Vives, P. Vachette, D. Durand and F. Fieschi, *J. Biol. Chem.*, 2009, **284**, 21229–21240.
43 M. Mayer and B. Meyer, *Angew. Chem., Int. Ed.*, 1999, **38**, 1784–1788.
44 J. Jeener, B. H. Meier, P. Bachmann and R. R. Ernst, *J. Chem. Phys.*, 1979, **71**, 4546–4553.
45 R. Wagner and S. Berger, *J. Magn. Reson., Ser. A*, 1996, **123**, 119–121.
46 G. Bains, R. T. Lee, Y. C. Lee and E. Freire, *Biochemistry*, 1992, **31**, 12624–12628.
47 *Maestro*, version 9.0, Schrödinger-LLC, New York, NY.
48 H. C. Kolb and B. Ernst, *Chem.–Eur. J.*, 1997, **3**, 1571–1578.
49 W. C. Still, A. Tempczyk, R. C. Hawley and T. Hendrickson, *J. Am. Chem. Soc.*, 1990, **112**, 6127–6129.
50 H. Feinberg, R. Castelli, K. Drickamer, P. H. Seeberger and W. I. Weis, *J. Biol. Chem.*, 2007, **282**, 4202–4209.
51 M. E. Taylor and K. Drickamer, *Glycobiology*, 2009, **19**, 1155–1162.
52 N. R. Krishna, D. G. Agresti, J. D. Glickson and R. Walter, *Biophys. J.*, 1978, **24**, 791–814.